International Journal of Engineering & Technology, 7 (4.18) (2018) 143-146

International Journal of Engineering & Technology

Website: www.sciencepubco.com/index.php/IJET

Research paper

AC Conductivity and Dielectric Properties of Strontium-Lead Borate Glasses

R. Hisam[1]*, A.K. Yahya[1], Dayana Said[1] M.F. Mustafa[2]

[1]*Faculty of Applied Sciences, Universiti Teknologi MARA, 40450 Shah Alam, Selangor, Malaysia*
[2]*Centre of Foundation Studies, Universiti Teknologi MARA, 48300 Dengkil, Selangor, Malaysia*
**Corresponding author E-mail: rosdiyana@salam.uitm.edu.my*

Abstract

The AC conductivity and dielectric properties of strontium-lead borate glasses with composition of (90-*x*)B_2O_3-10PbO-*x*SrO (*x* = 20, 25, 30, 35, 40, 45) were studied in the frequency range of 0.01 Hz to 10^6 Hz at room temperature to investigate the effects of SrO in the glasses. The variation of AC conductivity with SrO content showed a minimum value at *x* = 25 mol% before increasing to 25 < *x* ≤ 35 mol%, followed by a slight decrease of *x* > 35 mol%. Meanwhile, dielectric constant showed a minimum at *x* = 25 mol% before increasing to *x* > 25 mol%. The decrease at *x* = 25 mol% coincided with the σ_{AC} drop at the same concentration. This decrease could be associated with the increasing number of bridging oxygens, which restricted dipole movement. The electric modulus of the investigated samples showed that the trend of the imaginary part of the electrical modulus (*M″*) was in tandem with the behaviour of AC conductivity.

Keywords: *AC conductivity; borate glass; dielectric properties; electric modulus; impedance spectroscopy.*

1. Introduction

Glasses are the transparent and amorphous in nature that have been widely investigated due to their unique properties such as being isotropic and easy to fabricate and having excellent physical and chemical properties. The addition of oxides into glasses has been intensively studied due to their potential applications in many industrial fields such as optical amplifier media, tunable laser devices and outer space studies [1]. Based on the value of their single bond strength, oxides that are added to glasses could be classified as former, intermediate and modifier where high value of single bond strength could enhance glass-forming tendency [2]. Tellurite, silicate, germanate and borate are some examples of oxide glasses. Among them, borate, which is an excellent glass-forming material, has drawn special attention due to its attractive optical and physical properties and wide practical applications.

Boron trioxide(B_2O_3), is known as a very good glass network former, has excellent glass-forming ability due to its good resistace toward vibration, lower thermal expansion, high toughness, stress and chemical resistance as well as lower viscosity [3]. Interestingly, when alkaline oxide was introduces into borate glass, the additional oxygen from alkali oxide cause conversion from trigonal boron atom BO_3 into four-fold BO_4 coordinated boron [4]. By contrast, when alkali oxides are added to borate glass, non-linear behaviour were observed in the structural and physical. For instance, the density and glass transition temperature, T_g are increased with low concentration of alkali oxide. This anomalous behaviour is known as borate anomaly [5]. It is related to the conversion of sp2 planar [BO_3] units to stable sp^3 planar [BO_4] units and the possibility of creating non-bridging oxygen (NBO) [6].

Studies on binary *x*Li_2O-B_2O_3 glass system have revealed that addition of Li_2O up to *x* = 0.5 caused increasing of BO_4 corresponded to the increase in the number of bridging oxygen (BO). However, for *x* > 0.5, raman spectroscopy results further showed that increase in BO_3 indicated the the enhancement of NBO, which weakens the glass network [8]. Borate anomaly can also be observed when alkaline earth metal oxides such as CaO, SrO, MgO or BaO are added to borate glass [9,10]. By using mid-infrared spectra measurements, Yiannopoulos [9] reported that in *x*MO-(1-*x*)B_2O_3 (M = Ca, Sr, Ba), trigonal boron progressively changes to tetrahedral boron. Based on mid infrared (IR) spectra measurements, tetrahedral boron was found to decreased with SrO content (*x* ≤ 40 mol%) indicated to the increase in the number of NBO. Nevertheless, another study on binary SrO-B_2O_3 glasses showed that the changes in T_g may also be due to conversion of trigonal boron to tetrahedral boron. The addition of SrO into glass composition increases T_g until *x* = 40 mol% before decreasing after the concentration of SrO increases.

Meanwhile, the addition of alkaline earth oxide in ternary *x*BaO-(70-*x*)B_2O_3-10SiO_2 glass system showed T_g maximum at *x* = 30 mol % due to the change of coordination number of B, which was attributed to the transformation of BO_3 into BO_4 [11]. Interestingly, the dielectric properties of the glass system also showed dielectric anomaly at *x* = 30 mol% probably due to the high polarisability of Ba^{2+} ions. However, the dielectric constant only slightly decreases beyond 30 mol% of BaO and does not seem to be strongly affected by the borate anomaly. Nevertheless, this finding indicates that the borate anomaly not only affects the structural properties of the glasses but seems to also influence their dielectric properties. Thus, a more complete description of the borate anomaly should include the polarisation environment, which may be part of the nature of the anomaly.

Copyright © 2018 Authors. This is an open access article distributed under the Creative Commons Attribution License, which permits unrestricted use, distribution, and reproduction in any medium, provided the original work is properly cited.

On the other hand, the effect of SrO on the structural and elastic properties of SrO-PbO-B_2O_3 glasses was reported by Sabri et al. [10]. They found that the T_g maximum with SrO content which was due to the conversion of BO_3 and BO_4. The formation of BO_4 units contributes to improved rigidity of glass network, causing the increase of T_g. However, beyond 30 mol% of SrO, caused a slight decrease in T_g due to the increase in NBO, which implies a decrease in rigidity of the glass network. Hence, it would be interesting to investigate the AC conductivity and dielectric properties of (90-*x*)B_2O_3-10PbO-*x*SrO ternary glasses with increasing SrO concentration and fixed PbO concentration to further elucidate the anomalous behaviour of this glass system. Moreover, to the best of our knowledge, such studies on the *x*SrO-10PbO-(90-*x*)B_2O_3 glass system have not been conducted.

In this work, a series of (90-*x*)B_2O_3-10PbO-*x*SrO (*x* = 20, 25, 30, 35, 40, 45) glasses were studied to investigate the effect of SrO content on the AC conductivity and dielectric properties using impedance spectroscopy measurements.

2. Materials and methods

Glass samples with the molar composition (90-*x*)B_2O_3-10PbO-*x*SrO with *x* = 20, 25, 30, 35, 40, 45 (mol%) were successfully prepared through the melt-quenching method. The glass samples were initially mixing appropriate amounts of high-purity (>99.95%) powders of $SrCO_3$, PbO and B_2O_3. The mixture was homogenised using an agate mortar. The powder was melted in ceramic crucible at 1100 °C for 1 hour in a box furnace. The molten glass was the quenched to 300 °C in a pre-heated stainless-steel mould and annealed at 300 °C for 1 h to reduce the mechanical stresses of the quenched glass. The glass samples were polished using fine sand paper to a thickness of around 4.00 mm for impedance spectroscopy measurements.

Dielectric properties were determined using Solartron S1260A Impedance/Gain-Phase Analyzer over a frequency range of 10^{-2} to 10^6 Hz at room temperature. The dielectric constant (ε'), tan δ, and AC conductivity (σ_{ac}) were determined based on the following expressions:

$$\varepsilon' = Cd/\varepsilon_0 A \quad (1)$$

$$\varepsilon'' = \varepsilon' \tan\delta \quad (2)$$

$$\sigma_{ac} = \omega \varepsilon_0 \varepsilon'' \quad (3)$$

where ε_o is the permittivity constant of free space, C is the capacitance, ω is the frequency of the input signal, *d* is the thickness of the glass sample, and *A* is the cross-sectional are of the sample.

3. Results and discussion

3.1. AC conductivity

The amorphous nature of the (90-*x*)B_2O_3-10PbO-*x*SrO (*x* = 20, 25, 30, 35, 40, 45) glass samples was confirmed as previously reported [10]. Moreover, the structural effect of SrO on the same glass sample was investigated using FTIR spectroscopy, and the analysis reported the presence of BO_3 and BO_4 vibration groups. The study reported that the fraction of the four coordinated boron atoms (N4) increased for *x* < 30 mol% of SrO followed by a decrease of *x* > 30 mol% [10]. Fig. 1 shows the AC conductivity spectra for all glass samples at room temperature. The log σ_{ac} versus frequency profile can be separated into region 1 and region 2. In region 1, the plateau of log σ_{ac} in the medium frequency range, which become more visible at higher concentration of SrO corresponds to dc conductivity. The rapid decrease of conductivity at low frequencies for *x* = 25 mol% was suggested due to electrode polarization phenomenon. Meanwhile, at the higher frequency region (region 2), the conductivity varies strongly with frequency. The strong frequency dependent (region 2) indicates the presence of conductivity relaxation phenomenon [12].

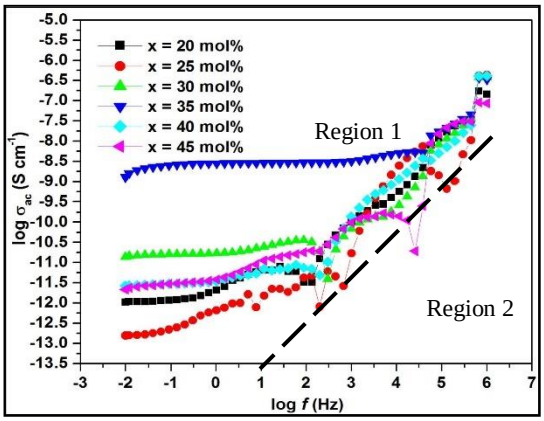

Fig.1: Plot of conductivities log (σ_{ac}) in the frequency domain at room temperature for (90-*x*)B_2O_3-10PbO-*x*SrO glass sample.

Fig. 2 shows an initial weak decrease of log σ_{ac} for $x \leq 25$ mol% before increasing steeply for $x > 25$ mol% until a maximum at $x = 35$ mol% and decreases beyond $x = 35$ mol%. The initial decrease of log σ_{ac} at $x \leq 25$ mol% (Fig. 2) can be attributed to the increase of BO with the addition of SrO. This indicated that the rigidity of the glass has increased, thus decreasing the mobility of Sr^{2+}. However, the conductivity later increased at $25 < x < 35$ mol% due to high polarisability of Sr ion. Moreover, PbO in this glass composition acted as modifier, opening the glass network and creating easier paths for charge carrier migration. For the region of $x > 35$ mol%, the conductivity decreased due to the increase of NBO atoms due to depolymerisation of borate glass. Depolymerisation causes partial opening of the network structure, which shortens the average chain length by breaking oxygen bonds that form bridges between the corners of the BO_4 tetrahedra [13]. This change in oxygen bonding leads to the increase of NBO concentration, which restricts the mobility of Sr ions.

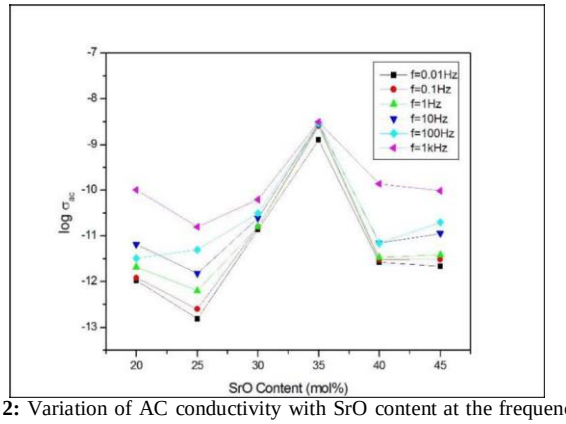

Fig. 2: Variation of AC conductivity with SrO content at the frequency of 0.01 Hz, 0.1 Hz, 1 Hz, 10 Hz, 100 Hz and 1 kHz.

3.2. Dielectric studies

The frequency dependence of dielectric constant, ε' of the glass samples at room temperature is shown in Fig. 3. From this figure, it can be seen that the variations of responses toward frequencies are almost similar for the glass samples except for when *x* = 35 mol%, where it become larger at low frequencies. The large increase in ε' at low frequency (*f* < 10 Hz) for *x* = 35 mol% is suggested to be due to the high contribution of ionic and orientation dipoles to the total polarizability [12]. In addition to at low frequencies, the contribution of space charge polarization is observed at lower frequencies, indicating that Sr ion contributed to the heavy dipole formation. This is caused by the increase of NBO that has weakened the glass network and the increase of the degree of deformation of glass network, further allowing the migration of

Sr ions that took part in the build-up of space charge polarisation and thus causing in the increase of ε'. The almost constant ε' at high frequency indicated that short-range displacement of ions may be involved and that the oscillations of dipoles were not impeded in this glass network.

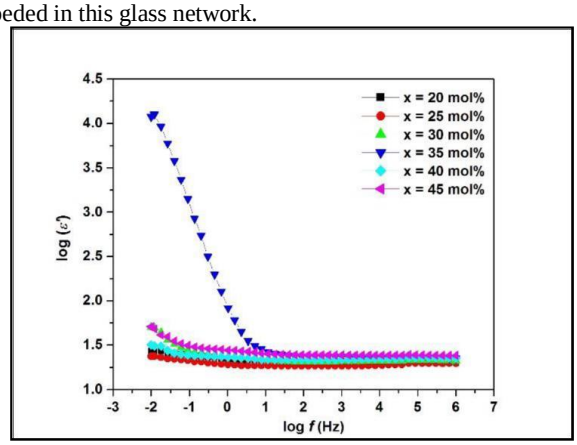

Fig. 3: Variation of dielectric constant (ε') with frequency at room temperature for the (90-*x*)B_2O_3-10PbO-*x*SrO (*x* = 20, 25, 30, 35, 40 and 45) glass samples.

Fig. 4 shows the variation of dielectric constant, ε' with SrO concentration measured for several frequencies at room temperature. The dielectric constant, ε', initially decreases for $x < 25$ mol% before increasing steeply for $x > 25$ mol%. The decrease in ε' at $x < 25$ mol% of SrO concentration was due to the increase of BO, which restricted dipole movement. For $x > 25$ mol%, ε' generally increases steeply due to high polarisability of Sr ion. In addition, the large increase in ε' values for $x > 25$ mol% indicated the effective delocalisation of heavy dipoles because of the NBO contributed by the BO_3 group and a decrease in the BO number by BO_4 functional group.

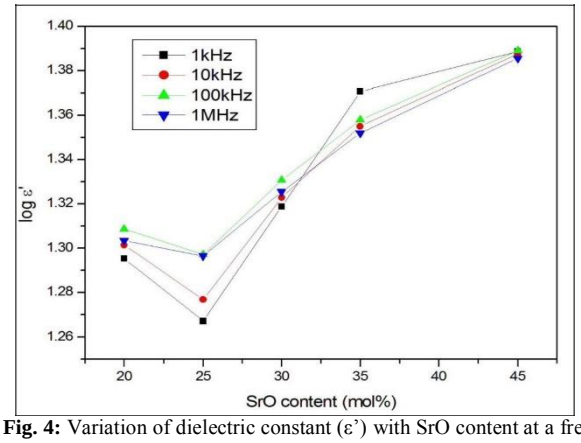

Fig. 4: Variation of dielectric constant (ε') with SrO content at a frequency of 1 kHz, 10 kHz, 100 kHz and 1 MHz at room temperature.

Fig. 5 shows the dielectric loss (tan δ) with frequency for all glass samples at room temperature. It is observed that the dielectric loss factor values are larger at low frequencies. The higher values at low frequencies can be attributed to the contribution of ion jump, DC conduction loss and electron polarization loss [14]. Moreover,the exhibited of a loss peak for $x = 35$ mol% at intermediate frequency indicated the relaxation process of heavy dipoles and may be due to the increase in dipolar interaction in the glass network.

Electrical responses of the glass samples were investigated by complex electrical modulus formalism, $M^*(\omega) = 1/\varepsilon^*(\omega)$ [15], where ε^* is the complex permittivity;

$$M^*(\omega) = \frac{1^*}{\varepsilon} = \varepsilon'/((\varepsilon')^2 + (\varepsilon'')^2) + i\varepsilon''/((\varepsilon')^2 + (\varepsilon'')^2) = M' + iM'' \quad (4)$$

Variation in the real part of electric modulus M' with the frequency obtained for all the composition of (90-*x*)B_2O_3-10PbO-*x*SrO glass samples at room temperature is shown in Fig. 6. From the figure it can be seen that the M' exhibited very small value at low frequencies for all glass samples except for $x = 25$ mol% which indicates a negligible or absent electrode polarization phenomenon and low migration energy barriers. The values of M' increase with increasing frequency, which indicated the start of relaxation process. At higher frequencies, the value of M' tends to saturate at M_∞ and forms a plateau region which attributed to the conduction phenomena due to short-range migration of charge carriers. Thus, it can be assumed that the motion of charge carrier was impeded and move only within their limited potential well [15]. The plateau region increases at $x > 25$ mol% but decreases for $x \geq 35$ mol%. The non-linear behaviour of M' with SrO content is similar to the trend of log σ_{ac} versus SrO concentration but in reverse manner. In addition, the high value of M' at $x = 25$ mol% of SrO can be attributed to its high electrical stiffness compared with other samples. For $x = 25$ mol%, the dispersion at low frequency was relatively larger than that of other glass samples, thereby indicating higher resistance to ionic carriers.

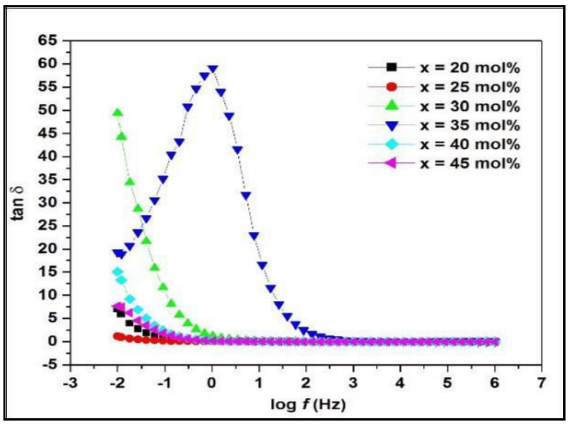

Fig. 5: Variation of tan δ with frequency at room temperature for the (90-*x*)B_2O_3-10PbO-*x*SrO (*x* = 20, 25, 30, 35, 40 and 45) glass samples.

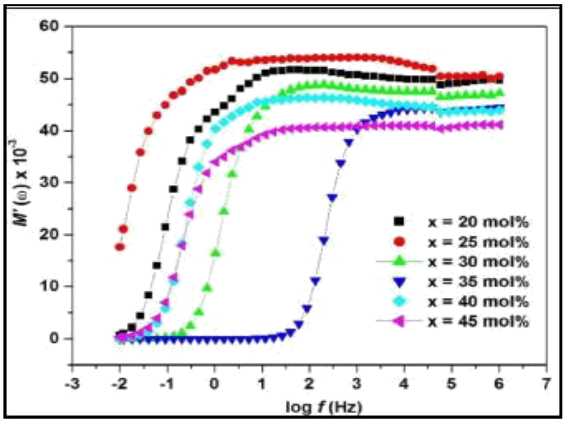

Fig. 6: Electric modulus *M*' as a function of log (*f*) plots for the (90-*x*)B_2O_3-10PbO-*x*SrO (*x* = 20, 25, 30, 35, 40 and 45) glass samples at room temperature.

Fig. 7 presents the M'' spectra for all composition at room temperature. From the figure, it can be observed that for $x < 25$ mol%, the peaks shift to lower frequency, and for $x \geq 30$ mol%, the peaks shifted to higher frequency until $x = 35$ mol% before shifting to low frequency for $x > 35$ mol%. This results indicate that electrical relaxation frequency is composition dependent. The trend of the M'' was in tandem with the behaviour of AC conductivity. Thus, the relaxation represented by the M'' peaks was related to the relaxation of charge carriers as previously suggested [13]. On the other hand, it is also observed from Fig. 7 that M'' (*f*) spectra consisted of an asymmetric maximum centered at the dispersion region of *M*' except for $x = 25$ mol%.

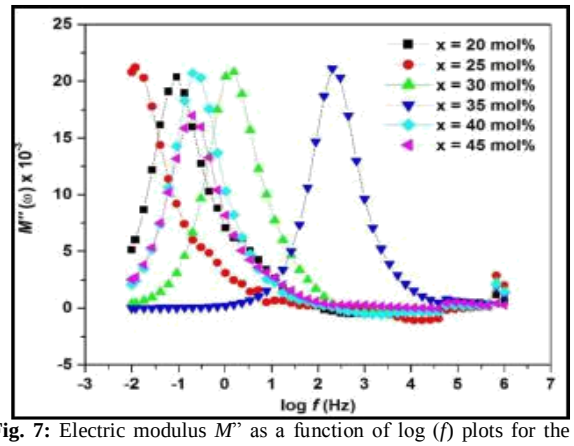

Fig. 7: Electric modulus *M*" as a function of log (*f*) plots for the (90-*x*)B_2O_3-10PbO-*x*SrO (*x* = 20, 25, 30, 35, 40 and 45) glass samples at room temperature.

4. Conclusion

The effects of SrO on the dielectric properties and AC conductivity of (90-*x*)B_2O_3-10PbO-*x*SrO glass was investigated. Both AC conductivity (σ_{AC}) and dielectric constant (ε') decreased to a minimum value at *x* = 25 mol%. The σ_{ac} and ε' minimum at *x* = 25 mol% were attributed to the increase in glass rigidity, thus decreasing the mobility of Sr^{2+} and restricting the movement of dipoles, respectively. However, at higher SrO additions, NBO formation resulted in the increase of σ_{AC} and ε'. The maximum value of electric modulus (*M'*) for *x* = 25 mol% at higher frequency coincided with the minimum of σ_{AC}. Meanwhile, the trend of the imaginary part of electric modulus, *M''*, was in tandem with the behaviour of σ_{AC}.

Acknowledgement

The authors would like to thank the Institute of Research Management and Innovation (IRMI) UiTM for the financial supports. The research is conducted at the Faculty of Applied Sciences, Universiti Teknologi MARA (UiTM), Malaysia under the support of LESTARI grant no: 600-IRMI/MyRA 5/3/LESTARI (043/2017).

References

[1] Abdel-Baki M and El-Diasty F (2006), Optical properties of oxide glasses containing transition metals: Case of titanium-and chromium-containing glasses. *Current Opinion in Solid State and Material Sciences* 10 (5-6), 217-229.

[2] Dimitrov V and Komatsu T (2013), Electronic polarizability, optical basicity and single bond strength of oxide glasses. *Journal of Chemical Technology and Metallurgy* 48, 549-554.

[3] Kaur G, Pandey OP and Singh K (2012). Effect of modifiers field strength on optical, structural and mechanical properties of lanthanum borosilicate glasses. *Journal of Non-Crystalline Solids* 358, 2589-2596.

[4] Khafagy AH, E-Adawy AA, Higazy AA, El-Rabaie S and Eid AS (2008), Studies of some mechanical and optical properties of (70-*x*)TeO_2+15B_2O_3+15P_2O_5+*x*Li_2O glasses. *Journal of Non-Crystalline Solids* 354, 3152-3158.

[5] Saddeek YB (2004), Structural analysis of alkali borate glasses. *Physica B: Condense Matter* 344, 163-175.

[6] Shelby JE (2005), Introduction to Glass Science And Technology, 2nd edition, Royal Society of Chemistry, Cambridge.

[7] Latif IAE (2005), Ultrasonic study on the role of Na_2O on the structure of Na_2O-B_2O_3 and Na_2O-B_2O_3-SiO_2 glasses. *Journal of Pure and Applied Ultrasonic* 27, 80-91.

[8] Kawashima M, Matsuda Y and Kojima S (2011), Temperature dependence of elastic properties in alkali borate binary glasses. *Journal of Molecular Structure* 993 (1-3), 155-159.

[9] Yiannopoulos Y, Chryssikos GD and Kamitsos E (2001), Structure and porperties of alkaline earth borate glasses. *Physics and Chemistry of Glasses* 42 (3),164-172.

[10] Sabri NS, Yahya AK, Abd Shukor R and Talari MK (2016), Anomalous elastic behaviour of *x*SrO-10PbO-(90-*x*)B_2O_3 glass system. *Journal of Non-Crystalline Solids* 444, 55-63.

[11] Eun-Sub L, Byung-Sook K, Joon-Hyung L and Jeong-Joo K (2007), Characterization of the low temperature firing BaO–B2O3–SiO2 glass: The effect of BaO content. *Journal of the European Ceramic Society* 27(2–3), 825-829.

[12] Abdel-Khalek EK, Mohamed EA, Shaaban M Salem and Kashif I (2018), Structural and dielectric properties of (100-*x*)B_2O_3-(*x*/2) Fe_2O_3 glasses and glass-ceramic containing $BiFeO_3$ phase. *Journal of Non-Crystalline Solids* 492, 41-49.

[13] Chaudhry MA and Bilal S (1995), Concentration-dependent electrical conductivity of phosphate glasses containing zinc oxide. *Materials Chemistry and Physics* 41(4), 299-301.

[14] Rosdiyana Hisam, Ahmad Kamal Yahya and Halimah Mohamed Kamari (2017), AC Conductivity and dielectric behavior in mixed electronic-ionic 30Li_2O-4MoO_3-(66-*x*)TeO_2-*x*V_2O_5 glass system. *Ionics* 23(6), 1423-1437.

[15] Rani S, Sanghi S, Ahlawat N and Agarwal A (2015), Influence of Bi_2O_3 on physical, electrical and thermal properties of Li_2O-ZnO-Bi_2O_3-SiO_2 glasses. *Journal of Alloy and Compound* 619, 659-666.